

Multiple hypothesis tracking based on the Shirayev sequential probability ratio test

Jinbin FU¹, Jinping SUN^{1*}, Songtao LU^{2*} & Yingjing ZHANG¹

¹*School of Electronic and Information Engineering, Beihang University, Beijing 100191, China;*
²*Department of Electrical and Computer Engineering, Iowa State University, Ames, IA 50011, USA*

Received October 3, 2015; accepted January 5, 2016; published online June 27, 2016

Abstract To date, Wald sequential probability ratio test (WSPRT) has been widely applied to track management of multiple hypothesis tracking (MHT). But in a real situation, if the false alarm spatial density is much larger than the new target spatial density, the original track score will be very close to the deletion threshold of the WSPRT. Consequently, all tracks, including target tracks, may easily be deleted, which means that the tracking performance is sensitive to the tracking environment. Meanwhile, if a target exists for a long time, its track will have a high score, which will make the track survive for a long time even after the target has disappeared. In this paper, to consider the relationship between the hypotheses of the test, we adopt the Shirayev SPRT (SSPRT) for track management in MHT. By introducing a hypothesis transition probability, the original track score can increase faster, which solves the first problem. In addition, by setting an independent SSPRT for track deletion, the track score can decrease faster, which solves the second problem. The simulation results show that the proposed SSPRT-based MHT can achieve better tracking performance than MHT based on the WSPRT under a high false alarm spatial density.

Keywords multiple target tracking, multiple hypothesis tracking, Shirayev sequential probability ratio test, track management, track score

Citation Fu J B, Sun J P, Lu S T, et al. Multiple hypothesis tracking based on the Shirayev sequential probability ratio test. *Sci China Inf Sci*, 2016, 59(12): 122306, doi: 10.1007/s11432-016-5570-4

1 Introduction

In the field of multiple target tracking, measurements from uncertain sources make data association difficult to perform [1, 2]. Using delayed decisions, multiple hypothesis tracking (MHT) algorithms can take advantage of additional measurements to eliminate the uncertainty of previous measurements in order to achieve better tracking performance [3]. But delayed decisions also result in tracks with more complex states, making track management more difficult. Fortunately, with the log likelihood ratio (LLR) of the track confirmation probability, called track score proposed in [4, 5], Wald sequential probability ratio test (WSPRT) [6, 7] can be applied to track management of MHT. Meanwhile, a new MHT algorithm called track-oriented MHT (TOMHT) was proposed in [8]. While traditional hypothesis-oriented MHT (HOMHT) maintains and predicts all existing global hypotheses at each scan [9], TOMHT regenerates

* Corresponding author (email: sunjinpings@buaa.edu.cn, songtao@iastate.edu)

global hypotheses based on the probability of current tracks at each scan. Since the number of hypotheses is usually one order of magnitude larger than the number of tracks [10], and the implementation of TOMHT is much easier than HOMHT [11], TOMHT typically runs faster than HOMHT. Hence, TOMHT is applied more widely than HOMHT in multiple target tracking.

The WSPRT can be used to manage tracks with either TOMHT or HOMHT. However, although the WSPRT has been proved to be efficient at most scenes in multiple target tracking, there are still some problems existing. First, the confirmation and deletion thresholds of the WSPRT are calculated based on the confirmation probability of the false track and deletion probability of the true track, which must be given by the user in advance. Hence, if the false alarm spatial density is much larger than the new target spatial density in a real situation, the track original score will be very close to the deletion threshold of the WSPRT. This will lead to all tracks, including target tracks, potentially being deleted at the beginning. Thus, the tracking performance is sensitive to the tracking environment. Second, a target track that exists for a long time will likely have a high score, which will make the track survive for a long time after the target has disappeared. An extra deletion mechanism is commonly utilized to solve this problem [12, 13]. But since tracks can also be deleted by the extra deletion mechanism, the deletion threshold of the WSPRT may not be reached. Since the threshold is calculated by the deletion probability of the true track, this will make the deletion probability of the true track unsatisfiable. Additionally, since the thresholds of track confirmation and deletion are both calculated by the deletion probability of the true track and the confirmation probability of the false track in the WSPRT, there is a strong relationship between track confirmation and deletion. However, this consistency is damaged by the extra mechanism which is utilized in the track deletion phase. Third, the WSPRT does not consider the relationship between the hypotheses of the test. At the track confirmation stage, the confirmation probability of a track should increase with the number of measurements associated with the track growing. Similar logic also holds for the track deletion stage.

Shiryayev SPRT (SSPRT) [14, 15], based on a Bayesian framework, has been used in maneuver detection problems [16]. In order to solve the above-mentioned problems of the WSPRT, this paper proposes to use the SSPRT for track management of MHT. First, regarding the relationship between the hypotheses of the test, the SSPRT introduces a hypothesis transition probability, which makes the low original score increase faster. This solves the early deletion problem. Meanwhile, similar to the use of an SSPRT to implement maneuver termination in [17] and track termination in [18], an extra SSPRT is used to delete tracks in this paper. To keep track deletion and confirmation being consistent, the deletion SSPRT in this paper is set to have the same logic as the confirmation SSPRT at the confirmation stage. In this way, the increases in the confirmation and deletion probability of false tracks caused by the hypothesis transition probability are equal, avoiding the problem where the hypothesis transition probability may lead to false tracks confirmed. The simulation of a formation targets scene shows that the SSPRT can get the same tracking performance as the WSPRT under the common condition and manage tracks better than the WSPRT in a high false alarm spatial density case. Furthermore, the method proposed in this paper can be applied to other improvements for MHT, like the factor graph [19].

2 Preliminaries

The track-orient MHT logic flowchart [13] is shown in Figure 1.

In Step 1, as a measurement z_k is detected at time k , a new track T_n is initialized with a confirmation probability, which equals

$$P(T_n) = \frac{\lambda_\nu}{\lambda_\phi + \lambda_\nu}, \quad (1)$$

where λ_ν is the new target spatial density and λ_ϕ is the false alarm spatial density. If the measurement can be associated to an existing track T_i whose confirmation probability is equal to $P(T_i)$, a track T_j will

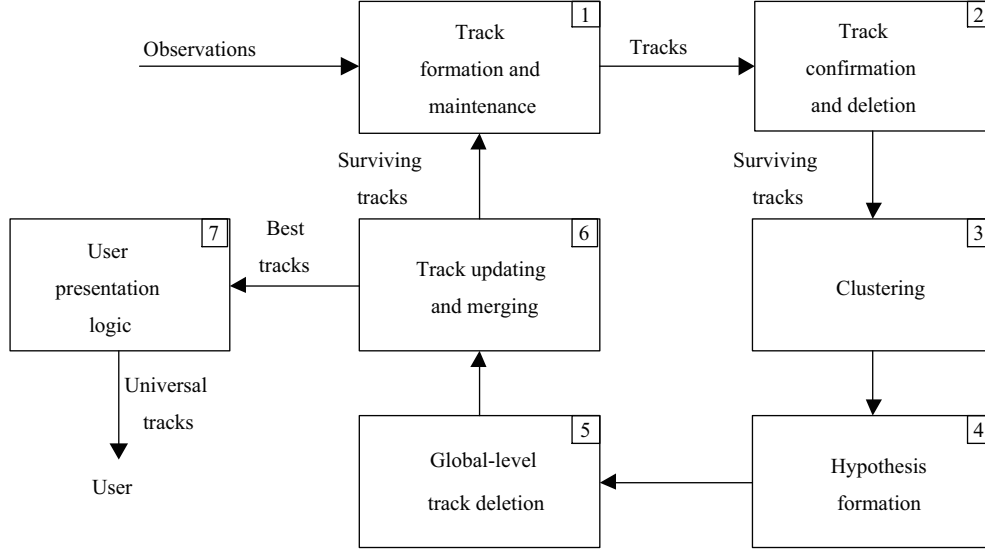


Figure 1 Track-oriented MHT logic flowchart.

be generated from the track T_i with a confirmation probability equal to [8]

$$P(T_j) = \frac{LR(z_k)P(T_i)}{[LR(z_k) - 1]P(T_i) + 1}, \quad (2)$$

where $LR(z_k)$ is the likelihood ratio that tests for classifying z_k as a measurement from T_i (H_1) versus a false alarm or a measurement from a new target (H_0), i.e.,

$$LR(z_k) = \frac{p(z_k | H_1)}{p(z_k | H_0)}. \quad (3)$$

The likelihood ratio of the measurement z_k can be calculated as in [13] as follows:

$$LR(z_k) = \frac{P_d p(z_k | T_i)}{\lambda_\phi + \lambda_\nu}, \quad (4)$$

where P_d is the detection probability and $p(z_k | T_i)$ is the probability that z_k is the measurement from the track T_i . Meanwhile, each existing track should generate a new track T_m which indicates that there are no measurements associated to them. The confirmation probability of T_m can be calculated by (2) as well, except with

$$LR(z_k) = 1 - P_d. \quad (5)$$

Here, i, j, n, m are indices used to identify different kinds of tracks.

However, instead of working with probabilities, it is more convenient to work with log-likelihood ratios called track score of the form

$$L_{T_j} = \ln \left[\frac{P(T_j)}{1 - P(T_j)} \right]. \quad (6)$$

Through (2), (4) and (5) and the conversion to the score by (6), the score for the track T_j can be computed recursively as

$$L_{T_j} = L_{T_i} + \ln[LR(z_k)], \quad (7)$$

where the initial score is given by

$$L_{T_n} = \ln[\lambda_\nu / \lambda_\phi]. \quad (8)$$

Besides, the confirmation probability can be calculated simply based on the track score by

$$P(T_i) = \frac{e^{L_{T_i}}}{e^{L_{T_i}} + 1}. \quad (9)$$

Since the track score is totally equivalent to the confirmation probability and the track score can be utilized more conveniently, the track-orient MHT just makes use of the track score instead of the confirmation probability during tracking.

In Step 2, the WSPRT, based on the track score, is performed as follows:

$$L_{T_i}(k) \begin{cases} \leq T_W^{d_1} = \ln \left[\frac{\beta}{1-\alpha} \right], & \text{delete the track,} \\ \geq T_W^c = \ln \left[\frac{1-\beta}{\alpha} \right], & \text{confirm the track,} \\ \in (T_W^{d_1}, T_W^c), & \text{defer decision,} \end{cases} \quad (10)$$

where $T_W^{d_1}$ is the deletion threshold of the WSPRT, T_W^c is the confirmation threshold of the WSPRT, α is the confirmation probability of the false track, and β is the deletion probability of the true track. Typically, $\alpha = 1 \times 10^{-6}$ and $\beta = 1 \times 10^{-3}$ [13].

We can observe that if λ_ϕ is three or more orders of magnitude larger than λ_ν , $\ln[\beta/1-\alpha]$ will be larger than $\ln[\lambda_\nu/\lambda_\phi]$, which means any track will be deleted immediately after they are initialized. In order to avoid the extreme case to happen, the tracks which are just initialized with the measurements received in the latest scan will not be judged whether they should be deleted or not. Unfortunately, even this way cannot solve the problem essentially, since the score increment from the next measurements may not be large enough to change the situation. Though the case that $\ln[\beta/1-\alpha]$ is much larger than $\ln[\lambda_\nu/\lambda_\phi]$ is not common, the case where $\ln[\lambda_\nu/\lambda_\phi]$ is very close to $\ln[\beta/1-\alpha]$ does occur often. This situation is precarious, since the score increment $\ln[LR(z_k)]$ in (2) is likely to be small or even less than zero because of a missed detection or a large covariance of target states when the track is newly initialized. This case will result in target tracks being deleted as well. On the other hand, if a target track exists for a long time, the score of this track will be very high based on (7) and (4). If only the deletion mechanism of the WSPRT is used, the track will then survive for a long time after the target has already disappeared, according to (7) and (5). Hence, an extra deletion mechanism may be added to handle this situation [12,13]. If the decrease of the score from the maximum score exceeds a threshold, the track will also be deleted, where the extra deletion threshold for the WSPRT can be selected as in [13], i.e.,

$$T_W^{d_2} = \ln \beta. \quad (11)$$

However, as mentioned above, the extra deletion mechanism not only makes the deletion probability of the true track unsatisfiable, but also damages the consistency between track confirmation and deletion in the WSPRT.

3 Multiple hypothesis tracking based on the Shirayev sequential probability ratio test

In order to solve the two problems of the WSPRT as mentioned above, the SSPRT is utilized. Since there are only two hypotheses in target tracking, i.e., the track is a target and the track is a false alarm, this paper limits discussion to the binary SSPRT.

The binary SSPRT assumes that hypothesis H_0 is true at the beginning of the test and a transition from H_0 to H_1 may occur. If the probability that the transition has occurred exceeds a specified threshold, the hypothesis H_1 is judged as true by the SSPRT. Let

$$p_k = P\{\theta \leq t_k | Z^k\} \quad (12)$$

denote the posterior probability that the transition occurs no later than time t_k given all available measurements Z^k , where θ is the time that the transition occurs.

In order to calculate p_k , based on the conditional probability formula, p_k can be calculated by

$$P\{\theta \leq t_k | Z^k\} = \frac{P\{Z^k | \theta \leq t_k\} P\{\theta \leq t_k\}}{P\{Z^k\}}. \quad (13)$$

Since $\{Z^{k-1} | \theta \leq t_k\}$ is independent with $\{z_k | \theta \leq t_k\}$, we can get

$$P\{Z^k | \theta \leq t_k\} = P\{Z^{k-1} | \theta \leq t_k\}P\{z_k | \theta \leq t_k\}. \tag{14}$$

Furthermore, using Bayesian theorem, we can have

$$P\{Z^{k-1} | \theta \leq t_k\} = \frac{P\{\theta \leq t_k | Z^{k-1}\}P\{Z^{k-1}\}}{P\{\theta \leq t_k\}}. \tag{15}$$

Meanwhile, according to the conditional probability and total probability formulas, we also have

$$P\{Z^k\} = P\{z_k | Z^{k-1}\}P\{Z^{k-1}\}, \tag{16}$$

$$P\{z_k | Z^{k-1}\} = P\{z_k | \theta \leq t_k\}P\{\theta \leq t_k | Z^{k-1}\} + P\{z_k | \theta > t_k\}P\{\theta > t_k | Z^{k-1}\}. \tag{17}$$

At last, since $P\{z_k | \theta \leq t_k\} = f_1(z_k)dz_k$ and $P\{z_k | \theta > t_k\} = f_0(z_k)dz_k$, where $f_i(z_k)$ is the probability density function (PDF) of z_k conditioned on H_i , based on equations from (13) to (17), we can obtain

$$P\{\theta \leq t_k | Z^k\} = \frac{f_1(z_k)P\{\theta \leq t_k | Z^{k-1}\}}{f_0(z_k)P\{\theta > t_k | Z^{k-1}\} + f_1(z_k)P\{\theta \leq t_k | Z^{k-1}\}}. \tag{18}$$

In order to simplify (18), an auxiliary function $\phi_i(k)$ is defined as

$$\phi_i(k) = \begin{cases} P\{\theta > t_{k+1} | Z^k\}, & i = 0, \\ P\{\theta \leq t_{k+1} | Z^k\}, & i = 1. \end{cases} \tag{19}$$

In particular, the function $\phi_1(k)$ can be calculated by

$$\begin{aligned} \phi_1(k) &= P\{\theta \leq t_{k+1} | Z^k\} \\ &= P\{\theta \leq t_k | Z^k\} + P\{\theta = t_{k+1} | \theta > t_k, Z^k\}P\{\theta > t_k | Z^k\} \\ &= p_k + \pi_k(1 - p_k), \end{aligned} \tag{20}$$

where π_k is the transition probability of H_0 to H_1 from k to $k+1$. Meanwhile, based on the definition

$$\phi_0(k) = 1 - \phi_1(k), \tag{21}$$

we have p_k which can be calculated as

$$p_k = \frac{\phi_1(k-1)f_1(z_k)}{\sum_{i=0}^1 \phi_i(k-1)f_i(z_k)} = \frac{\phi_1(k-1)f_1(z_k)}{\phi_1(k-1)f_1(z_k) + (1 - \pi_k)(1 - p_{k-1})f_0(z_k)}. \tag{22}$$

Hence, we can obtain p_k in the score form for MHT as follows:

$$L_{T_i} = \ln \left[\frac{p_k}{1 - p_k} \right] = \ln \left[\frac{e^{L_{T_i}(k-1)} + \pi_k}{1 - \pi_k} \right] + \ln[LR(z_k)], \tag{23}$$

where

$$LR(z_k) = f_1(z_k)/f_0(z_k). \tag{24}$$

Since the $LR(z_k)$ defined in (24) is also a likelihood ratio of z_k under the same two hypotheses, Eq. (24) is equivalent to (3) in essence.

Since an initialized track could be either a false alarm or a target, and one binary SSPRT can only implement either track confirmation or deletion, two independent SSPRTs are necessary. One of them is used to confirm tracks and the other is used to delete tracks. The confirmation and deletion SSPRTs are defined in Table 1.

In Step 1 in Figure 1, as a measurement z_k is detected, a new track is initialized with scores for both the confirmation SSPRT and deletion SSPRT, which are denoted by

$$L_{T_i}^c = \ln[\lambda_\nu/\lambda_\phi], \quad L_{T_i}^d = \ln[\lambda_\phi/\lambda_\nu]. \tag{25}$$

Table 1 Definitions of confirmation and deletion SSPRTs

SSPRT	H_0	H_1
Confirmation SSPRT	The track is a false alarm	The track is a target
Deletion SSPRT	The track is a target	The track is a false alarm

If the measurement z_k can be associated to the track T_i , the scores of the confirmation SSPRT and deletion SSPRT can be calculated by (23) with respect to the score at last time, where $LR(z_k)$ in the confirmation SSPRT can be calculated by (4), and $LR(z_k)$ in the deletion SSPRT is the reciprocal of (4). As to the tracks which indicate that there are no measurements associated, $LR(z_k)$ in the confirmation SSPRT equals $1 - P_d$, and $LR(z_k)$ in the deletion SSPRT is the reciprocal of $1 - P_d$.

In Step 2 in Figure 1, the SSPRT is performed as follows:

- (1) At the confirmation stage, if the confirmation SSPRT exceeds the confirmation threshold, the track will be confirmed.
- (2) Otherwise, if the deletion SSPRT exceeds the deletion threshold, the track will be deleted.
- (3) If the track is confirmed, the confirmation SSPRT will be removed, but the deletion SSPRT will remain until the track is deleted.
- (4) If the track is deleted at the confirmation stage, both SSPRTs will be removed.

The thresholds of the confirmation and deletion SSPRTs can be calculated based on the threshold of track confirmation probability ξ and the threshold of the track deletion probability ζ , which are given by the user in advance. Then, we can choose them as

$$T_S^c = \ln \left[\frac{\xi}{1 - \xi} \right], \quad T_S^d = \ln \left[\frac{\zeta}{1 - \zeta} \right]. \quad (26)$$

In order to make the confirmation SSPRT and deletion SSPRT consistent with each other, ζ should be equal to ξ .

Finally, hypothesis transition probabilities are designed as follows. In order to describe the relationship between the hypotheses of the test at the confirmation stage, the hypothesis transition probability of the confirmation SSPRT π_k^c can be calculated by

$$\pi_k^c = 1 - e^{-(n_m - 1)/l_{ps}}, \quad n_m \geq 1, \quad (27)$$

where n_m is the number of measurements which has been associated to the track and l_{ps} is the expected scan number for target confirmation. The value of $n_m = 1$ indicates that the track has just been initialized, so π_k^c is set to zero. Since the relationship between π_k^c and n_m follows the geometric distribution [18], π_k^c is set to be exponentially increased with n_m . Finally, since the π_k^c is between 0 and 1, the π_k^c in this paper is calculated by one minus $e^{-(n_m - 1)/l_{ps}}$. But, in this way, the false tracks are difficult to be deleted as well, which affects the performance of deletion for false tracks. In order to solve this problem, the hypothesis transition probability of the deletion SSPRT π_k^d is set to equal π_k^c . In this way, although the confirmation probabilities of false tracks increase because of the hypothesis transition probability, the deletion probabilities of false tracks increase with the same speed as well. If a track is a false track, the difference between the track score increment $\ln[LR(z_k)]$ of the two SSPRTs will make the deletion SSPRT exceed the threshold first, such that the false track can be deleted.

When the track has been confirmed, the hypothesis transition probability of the deletion SSPRT changes to

$$\pi_k^d = \begin{cases} 1 - e^{-(n_{md} - n_e)/\sigma}, & n_{md} \geq n_e, \\ 0, & n_{md} < n_e, \end{cases} \quad (28)$$

where n_{md} denotes the number of miss detections in the last N scans, n_e denotes the expected number of miss detections in the last N scans, and σ is the standard variance of n_{md} . Since n_{md} is binomially distributed, we have

$$n_e = \lceil (1 - P_d)N \rceil, \quad (29)$$

$$\sigma = \sqrt{P_d(1 - P_d)N}. \quad (30)$$

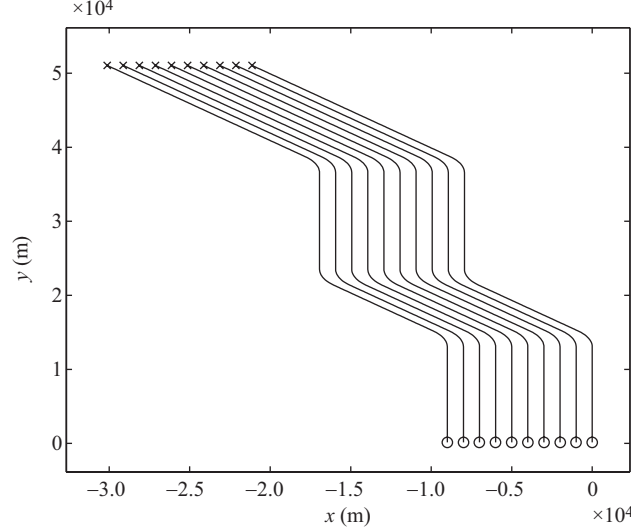


Figure 2 Formation targets scene. Start/Stop positions are marked with o/x.

Here, n_e is set to equal $\lceil (1 - P_d)N \rceil$ because of these following reasons. First, the n_{md} must be an integer, so n_e should be an integer as well. Otherwise, the case of $n_{md} \geq n_e$ will occur often in normal situations such that π_k^d is larger than zero and the tracks are deleted falsely. Second, it is inappropriate to make some limitations on P_d and N . At last, it is acceptable to make this approximation since it will just put off the tracks being deleted for a while and the performance of the SSPRT with this approximation is still better than that of the WSPRT in any case.

4 Performance evaluation

In order to verify the performance of the SSPRT for track management, TOMHT based on the SSPRT (S-TOMHT) is compared with TOMHT based on the WSPRT (W-TOMHT). The extra deletion mechanism is utilized in W-TOMHT. We select the formation target scene, similar as in [12], shown in Figure 2 where the clutter measurements are not shown. In this scene, 10 targets are moving in a formation, where each target is separated apart from its neighbors with 1000 m and maintains the speed 300 m/s over a period of 200 s. Each target performs three $3g$ (g is the gravitational acceleration) coordinate turns at 44, 81 and 132 s, each one lasting for 8 s and with a course change of 45° .

The target motion model is assumed to be a continuous white noise acceleration model with the following state equation:

$$\mathbf{X}_n = \mathbf{F}\mathbf{X}_{n-1} + \mathbf{w}_n, \tag{31}$$

where

$$\mathbf{X}_n = [x(n), y(n), \dot{x}(n), \dot{y}(n)]^T, \tag{32}$$

$$\mathbf{F} = \begin{bmatrix} 1 & 0 & T & 0 \\ 0 & 1 & 0 & T \\ 0 & 0 & 1 & 0 \\ 0 & 0 & 0 & 1 \end{bmatrix}, \tag{33}$$

where T is the sample interval. The process noise \mathbf{w}_n is zero-mean Gaussian with a covariance matrix

$$\mathbf{Q}_n = \begin{bmatrix} T^3/3 & 0 & T^2/2 & 0 \\ 0 & T^3/3 & 0 & T^2/2 \\ T^2/2 & 0 & T & 0 \\ 0 & T^2/2 & 0 & T \end{bmatrix} \tilde{q}, \tag{34}$$

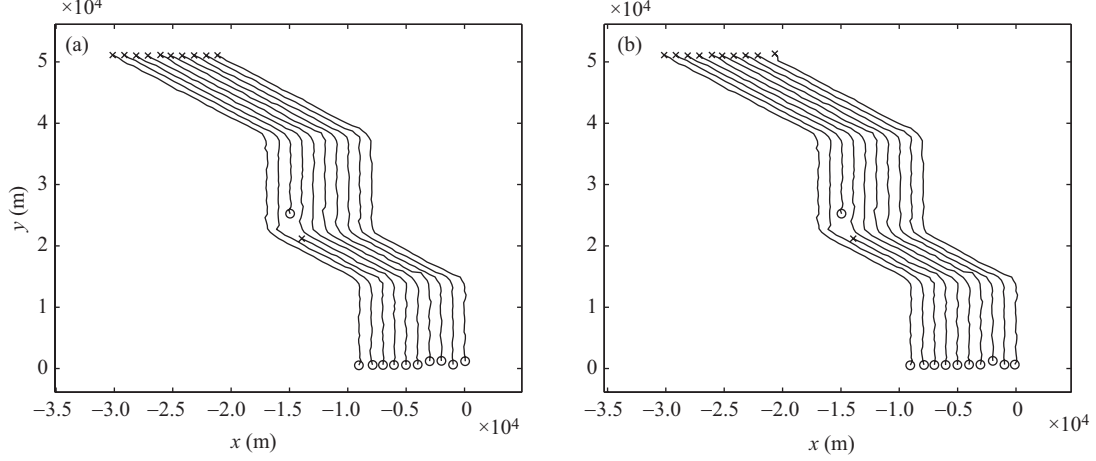


Figure 3 Tracking results of 50 Monte Carlo simulations with $\lambda_\phi = 6 \times 10^{-9}/\text{m}^2$. (a) W-TOHMT; (b) S-TOHMT.

where \tilde{q} is the power spectral density (PSD) of the continuous time white noise that models the motion uncertainty. The measurement model is defined as

$$\mathbf{Z}_n = \mathbf{H}\mathbf{X}_n + \mathbf{v}_n, \quad (35)$$

where

$$\mathbf{H} = \begin{bmatrix} 1 & 0 & 0 & 0 \\ 0 & 1 & 0 & 0 \end{bmatrix}. \quad (36)$$

The measurement noise \mathbf{v}_n is zero-mean Gaussian with covariance matrix

$$\mathbf{R}_n = \begin{bmatrix} \sigma_x^2 & 0 \\ 0 & \sigma_y^2 \end{bmatrix}. \quad (37)$$

Further we assume that the process noise and the measurement noise are mutually uncorrelated.

During the numerical simulations, the detection probability is set to $P_d = 0.9$ and the new target spatial density is $\lambda_\nu = 1 \times 10^{-11}/\text{m}^2$. The depth of TOMHT equals 5, and the sample interval T is equal to 2 s. The PSD and measurement noise standard variance are $\tilde{q} = 500 \text{ m}^2/\text{s}^3$ and $\sigma_x = \sigma_y = 50 \text{ m}$ respectively. In the WSPRT, the confirmation probability of the false track is $\alpha = 1 \times 10^{-6}$ and the deletion probability of the true track is $\beta = 1 \times 10^{-3}$ [13]. In the SSPRT, the thresholds of the track confirmation and deletion probabilities are $\xi = \zeta = 0.9$. The expected scan number for target confirmation is $l_{ps} = 3$, and the length of the scan window is $N = 10$. Meanwhile, as mentioned above, the tracks which are just initialized with the measurements received in the latest scan will not be judged whether they should be deleted or not.

First, in order to verify the performance of S-TOMHT under the common condition, the false alarm spatial density is set to be $\lambda_\phi = 6 \times 10^{-9}/\text{m}^2$. The tracking results are shown in Figure 3.

Based on the simulation results, we can observe that both of the W-SPRT and the S-SPRT can obtain good performance under the common condition and the tracking performance of S-TOMHT is almost the same as that of W-TOMHT.

Then, the false alarm spatial density is set to $\lambda_\phi = 6 \times 10^{-8}/\text{m}^2$. In order to compare the performances of the two trackers better, some extra performance metrics are selected which are defined the same as Ref. [12].

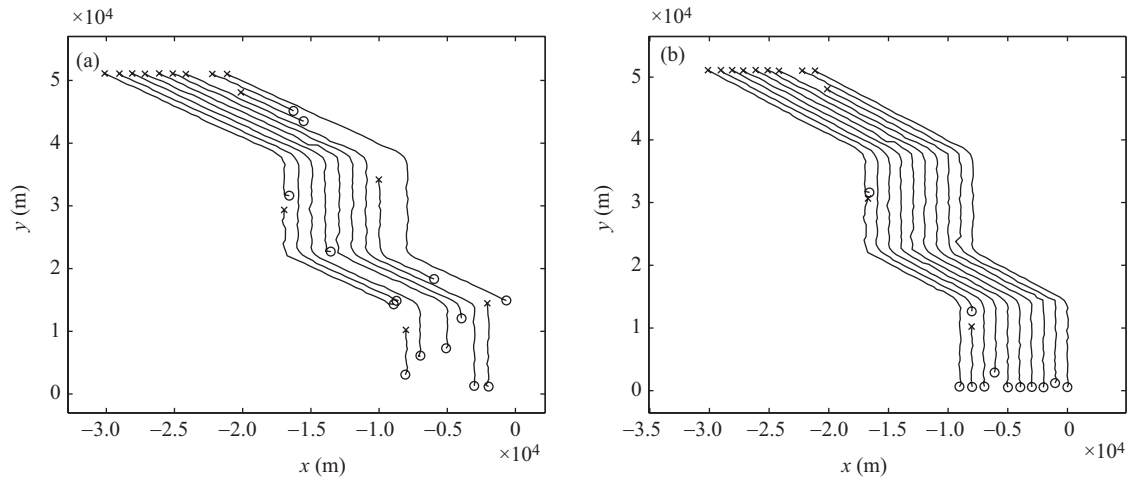
(1) Number of true tracks reported by a tracker (N_T). A track is defined as a “true track” when more than 50 percent of the track’s measurements originate from the same target.

(2) Number of false tracks reported by the tracker (N_F). A track that is not a true track is considered as a false track.

(3) True track life (L_T). Track life is defined as the duration of a track measured in number of scans. The maximum, minimum and average life of true tracks are considered in this paper.

Table 2 Simulation results of the formation target scene with $\lambda_\phi = 6 \times 10^{-8}/\text{m}^2$

Tracker	N_T	N_F	L_T			L_F		
			Max.	Min.	Avg.	Max.	Min.	Avg.
W-TOMHT	11.52	0.12	95.64	17.72	61.98	8.04	8.04	8.04
S-TOMHT	13.36	0.06	99.14	18.34	72.95	4.04	4.04	4.04

**Figure 4** Tracking results of 50 Monte Carlo simulations with $\lambda_\phi = 6 \times 10^{-8}/\text{m}^2$. (a) W-TOMHT; (b) S-TOMHT.

(4) False track life (N_F). Life of false tracks reported by a tracker is also measured in number of scans. The maximum, minimum and average life of false tracks are considered in this paper.

The results of 50 Monte Carlo simulations are shown in Table 2 and Figure 4.

First, we can observe that the number of true tracks reported by S-TOMHT is more than W-TOMHT, and that both of them are more than the actual number of targets, giving the impression that the tracks of S-TOMHT have more track breaks. But in Figure 4, we can see that W-TOMHT cannot re-initialize the target track after the track breaks. This also can be explained by the average true track life of S-TOMHT being larger than that of W-TOMHT. In terms of false track initialization, there are only three false tracks totally initialized by S-TOMHT in 50 Monte Carlo simulations, which is less than six by W-TOMHT. Since only one track is initialized each time, the average values for the maximum, minimum and mean false track life in 50 Monte Carlo simulations are equal.

On the other hand, the maximum and average values of true track life of S-TOMHT are larger than those of W-TOMHT. This means that S-TOMHT can maintain true tracks better than W-TOMHT. Additionally, the maximum, minimum and average values of false track life of S-TOMHT are less than those of W-TOMHT, which indicates that S-TOMHT can delete false tracks faster.

Finally, the overall tracking performance is compared in terms of the optimal subpattern assignment (OSPA) distance [20]. The OSPA distance between the two sets $X = \{x_1, x_2, \dots, x_m\}$ and $\hat{X} = \{\hat{x}_1, \hat{x}_2, \dots, \hat{x}_n\}$ is defined as

$$d_{\text{OSPA}}^{(c)}(X, \hat{X}) \triangleq \left(\frac{1}{n} \left(\min_{\pi \in \prod_n} \max_{1 \leq i \leq n} d^{(c)}(x_i, \hat{x}_{\pi(i)})^p + c^p(n-m) \right) \right)^{1/p}, n \geq m. \quad (38)$$

If $n \leq m$, we have $d_{\text{OSPA}}^{(c)}(X, \hat{X}) \triangleq d_{\text{OSPA}}^{(c)}(\hat{X}, X)$. Here \prod_n denotes the set of all possible permutations of $\{1, 2, \dots, n\}$ and $d^{(c)}(x, \hat{x}) \triangleq \min(c, d(x, \hat{x}))$ represents the truncated Euclidean distance between vectors x and \hat{x} . The cut-off distance c is set to 5000 and the order parameter p is fixed at 2. The simulation results are shown in Figure 5.

Since the filter can give more and more accurate estimation as the filtering proceeds, the OSPA distance of W-TOMHT decreases at the beginning of filtering, but the OSPA distance of S-TOMHT decreases to a lower amount in less time. Since the maneuvers make filtering accuracy decrease and false association rate increase, the OSPA distance of S-TOMHT has several fluctuations within a narrow range, similar to

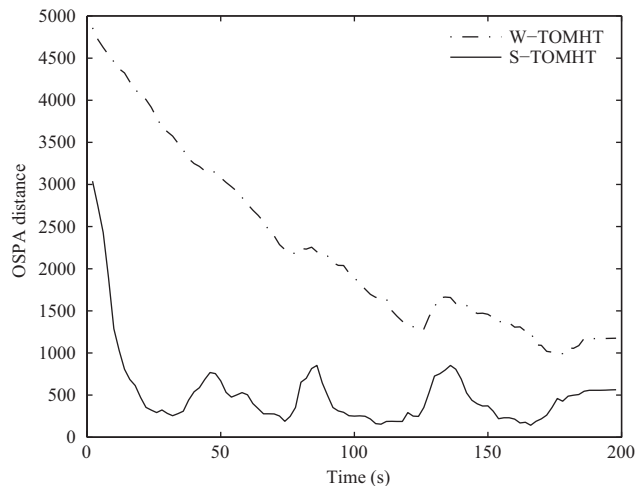


Figure 5 OSPA distance of the formation targets scene with $p = 2$, $c = 5000$.

W-TOMHT. But in general, the tracking performance of S-TOMHT is much better than W-TOMHT in terms of the OSPA distance.

5 Conclusion

Due to two problems when the WSPRT is applied to track management of MHT, this paper explores the substitution of the SSPRT for the WSPRT. To consider the relationship between the hypotheses of the test, the SSPRT introduces the hypothesis transition probability, which not only adapts to a real situation better, but also solves an issue for the WSPRT in which the tracking performance is sensitive to the tracking environment. Meanwhile, two independent SSPRTs are used to confirm and delete tracks, making track confirmation and deletion consistent with each other. Through numerical simulations on a formation targets scene under a high false alarm spatial density, it has been shown that TOMHT based on the SSPRT not only can initialize true tracks faster, with less false tracks being initialized, but also can maintain true tracks better with false tracks being deleted faster. In terms of overall tracking performance, TOMHT based on the SSPRT is considerably better than TOMHT based on the WSPRT.

Acknowledgements This work was supported by National Natural Science Foundation of China (Grant Nos. 61471019, 61501011).

Conflict of interest The authors declare that they have no conflict of interest.

References

- 1 Chavali P, Nehorai A. Concurrent particle filtering and data association using game theory for tracking multiple maneuvering targets. *IEEE Trans Signal Proc*, 2013, 61: 4934–4948
- 2 Taek S L, Dong L G. A probabilistic nearest neighbor filter algorithm for m validated measurements. *IEEE Trans Signal Proc*, 2006, 54: 2797–2802
- 3 Frank A, Smyth P, Ihler A. Beyond MAP estimation with the track-oriented multiple hypothesis tracker. *IEEE Trans Signal Proc*, 2014, 62: 2413–2423
- 4 Sittler R W. An optimal data association problem in surveillance theory. *IEEE Trans Mil Electron*, 1964, 8: 125–139
- 5 Stein J J, Blackman S S. Generalized correlation of multitarget track data. *IEEE Trans Aerosp Electron Syst*, 1975, 11: 1207–1217
- 6 Niu R, Varshney P K. Sampling schemes for sequential detection with dependent observations. *IEEE Trans Signal Proc*, 2010, 58: 1469–1481
- 7 Suratman F Y, Zoubir A M. Bootstrap based sequential probability ratio tests. In: *Proceedings of IEEE International Conference on Acoustics, Speech, Signal Process (ICASSP'13)*, Vancouver, 2013. 6352–6356
- 8 Demos G C, Ribas R A, Broida T J, et al. Applications of MHT to dim moving targets. In: *Proceedings of the Society of Photo-Optical Instrumentation Engineers (SPIE) Conference Series*, Los Angeles, 1990. 297–309
- 9 Reid D B. An algorithm for tracking multiple targets. *IEEE Trans Automat Contr*, 1979, 24: 843–854

- 10 Blackman S S. Multiple hypothesis tracking for multiple target tracking. *IEEE Aerosp Electron Syst*, 2004, 19: 5–18
- 11 Bar-Shalom Y, Blackman S S, Fitzgerald R J. Dimensionless score function for multiple hypothesis tracking. *IEEE Trans Aerosp Electron Syst*, 2007, 43: 392–400
- 12 Ren X Y, Luo T J, Huang Z P, *et al.* An efficient MHT implementation using GRASP. *IEEE Trans Aerosp Electron Syst*, 2014, 50: 86–101
- 13 Blackman S S, Popoli R. *Design and Analysis of Modern Tracking Systems*. London: Artech House, 1999
- 14 Shiryaev A N. *Optimal Stopping Rules*. New York: Springer-Verlag, 1977
- 15 Malladi D P, Speyer J L. A generalized Shiryaev sequential probability ratio test for change detection and isolation. *IEEE Trans Automat Contr*, 1999, 44: 1522–1534
- 16 Ru J, Jilkov V P, Li X R, *et al.* Detection of target maneuver onset. *IEEE Trans Aerosp Electron Syst*, 2009, 45: 536–554
- 17 Yu L, Li X R. Sequential multiple-model detection of target maneuver termination. In: *Proceedings of the 14th International Conference on Information Fusion (FUSION)*, Chicago, 2011. 1–8
- 18 Blanding W R, Willett P K, Bar-Shalom Y, *et al.* Multisensor track management for targets with fluctuating SNR. *IEEE Trans Aerosp Electron Syst*, 2009, 45: 1275–1292
- 19 Wang H, Sun J P, Lu S T, *et al.* Factor graph aided multiple hypothesis tracking. *Sci China Inf Sci*, 2013, 56: 109301
- 20 Schuhmacher D, Vo B T, Vo B N. A consistent metric for performance evaluation of multiobject filters. *IEEE Trans Signal Proc*, 2008, 56: 3447–3457